


Article

Rate-Based Modeling and Assessment of an Amine-Based Acid Gas Removal Process through a Comprehensive Solvent Selection Procedure

Neha Agarwal [†], Le Cao Nhien [†]  and Moonyong Lee ^{*} 

School of Chemical Engineering, Yeungnam University, Gyeongsan 38541, Korea

^{*} Correspondence: mynlee@yu.ac.kr; Tel.: +82-53-810-2512[†] These authors contributed equally to this work.

Abstract: In this study, an industrial acid gas removal (AGR) process which uses amine-based solvents was designed and simulated. The selection of suitable absorbents is crucial for an effective AGR process. Therefore, various single and blended amine-based solvents for capturing acid gases were evaluated through a comprehensive procedure, including solvent screening and process design steps. First, various solvents were screened for their CO₂ and H₂S absorption efficiencies. Promising solvents were then selected for the process design step, in which all process alternatives were simulated and rigorously designed using Aspen Plus. The non-equilibrium rate-based method with an electrolyte non-random two-liquid thermodynamic model was employed for modeling the absorption column. All processes were evaluated in terms of energy requirements, costs, and carbon emissions. The results show that a blend of methyldiethanolamine and piperazine solutions are the most promising solvents for the AGR process, as they can save up to 29.1% and 30.3% of the total annual costs and carbon emissions, respectively, compared to the methyldiethanolamine + diethanolamine solvent process.

Keywords: acid gas removal; process simulation; chemical absorption; rate-based approach; blended amines; Aspen Plus



Citation: Agarwal, N.; Cao Nhien, L.; Lee, M. Rate-Based Modeling and Assessment of an Amine-Based Acid Gas Removal Process through a Comprehensive Solvent Selection Procedure. *Energies* **2022**, *15*, 6817. <https://doi.org/10.3390/en15186817>

Received: 12 July 2022

Accepted: 15 September 2022

Published: 18 September 2022

Publisher's Note: MDPI stays neutral with regard to jurisdictional claims in published maps and institutional affiliations.



Copyright: © 2022 by the authors. Licensee MDPI, Basel, Switzerland. This article is an open access article distributed under the terms and conditions of the Creative Commons Attribution (CC BY) license (<https://creativecommons.org/licenses/by/4.0/>).

1. Introduction

Environmental degradation is a critical issue that requires urgent scientific attention. Carbon dioxide (CO₂) is the dominant anthropogenic greenhouse gas. The emission of CO₂ from industrial activities, which have continued to grow rapidly, is the main driver of global warming. Global warming benchmarks of 1.5 and 2 °C are predicted to be exceeded during the 21st century, which is considered an alarming situation [1]. Global CO₂ emissions in 2021 were recorded as the highest ever. Figure 1 presents the CO₂ concentration in the atmosphere from 1958 to the present; as of May 2022, atmospheric CO₂ concentration reached 418 ppm. In particular, CO₂ emissions from power plants are the highest recorded, accounting for 46% of the global increase in emissions [2]. Fortunately, more than 90% of CO₂ emissions from power plants and industrial facilities can be captured by applying carbon capture (CC), use, and storage technologies [3]. Therefore, interest in CO₂ capture technologies, which are the only practical way to attain long-term CO₂ reduction targets, has increased significantly in recent years and should be applied in large power plants and industries. The main challenge is to determine the most cost- and an energy-efficient possible route for the CO₂ capture process.

In recent decades, various types of technologies have been developed to reduce CO₂ emissions. Currently, there are three main methods of CC: pre-combustion CC, post-combustion CC, and oxyfuel CC. Of these, post-combustion CC is the most widely used because of its high selectivity and low energy consumption [4]. This technique is explicitly gaining attention because it can be built separately or retrofitted to an existing plant [5].

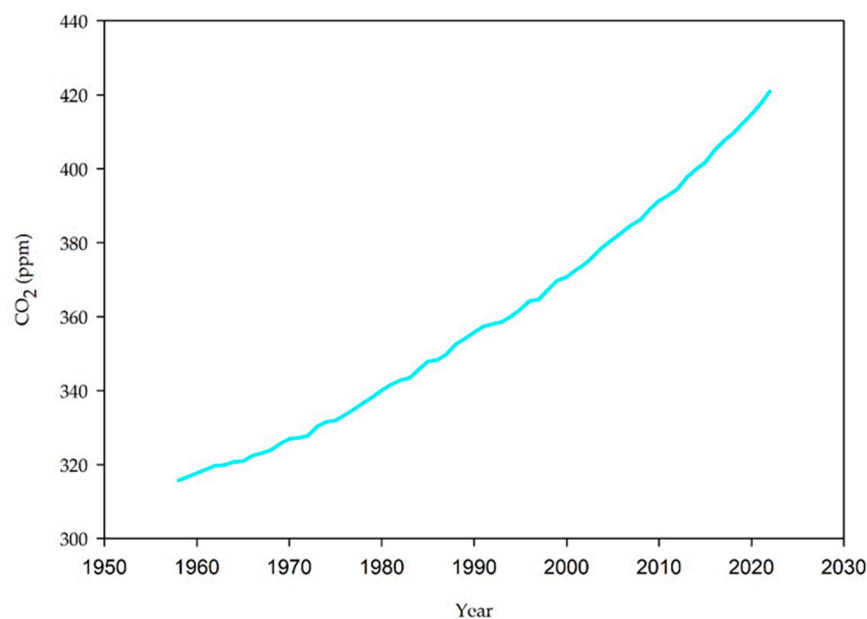


Figure 1. Atmospheric CO₂ levels.

In general, post-combustion CC techniques could be divided into physical and chemical methods. In the physical method, which includes membrane separation, cryogenic condensation, and physical absorption technologies, CO₂ is removed from flue gas by organic solution without chemical reaction. On the other hand, chemical absorbents react with CO₂ to remove it from flue gas in the chemical method. Its main technologies are chemical absorption, adsorption, and looping combustion. As compared to physical absorption, chemical absorption has several advantages, such as mature technology, high efficiency, and low cost [6]. In particular, CA or reactive absorption using chemical solvents as absorbents is the most frequently used and commercially available technology for gas treatment [7]. In the CA process, the absorption of components can occur simultaneously in the liquid phase; thus, it requires a lower solvent flow rate and pressure than the physical absorption process [7].

Commonly used chemical absorbents include amines, ammonia, potassium carbonate, and sodium hydroxide [4]. Several studies have been carried out using a single solution, whereas others have been carried out using a blended solution under different operational conditions. Research has recently focused on applying new energy-effective absorbents [8]. Various amine-based solvents, including single and blended solvents, have been studied under various operating conditions [9–11]. The addition of amines significantly affects the solubility of CO₂ and H₂S in water [12]. Amine-based solvents have also been observed to have a high separation efficiency, with the rate of CO₂ removal affected by the solvent temperature and flow rate [13].

For primary and secondary amines, the maximum possible CO₂ loading is one mole of CO₂ per two moles of amine, with the formation of zwitterions and carbamates. However, for tertiary amines, this limit decreases to one mole of CO₂ per mole of amine with the formation of bicarbonates [14]. Esmaeili et al. evaluated various single solvents, such as diethanolamine (DEA), methyldiethanolamine (MDEA), and blended amine solvents of piperazine (PZ) and MDEA at different concentrations, for CO₂ absorption from the ethane stream [15]. The authors concluded that a blended solution of 1 wt% PZ and 39 wt% MDEA, which resulted in maximum CO₂ loading, was the most promising absorbent for the studied process. Kalatjari et al. employed Aspen Plus to model the CO₂ capture process using the monoethanolamine (MEA) solvent at various concentrations with different thermodynamic models [16]. Therefore, amines are considered highly effective absorbents, which are attracting greater attention. Recent studies have focused on developing blended solvents, i.e., blending a primary or secondary amine with a tertiary amine or carbonate, to improve

the CO₂ absorption rate [17]. In particular, MEA or diethanolamine (DEA) can be mixed with an MDEA solution to enhance the absorption efficiency without increasing the energy requirement in the regenerator step [17]. In this study, a tertiary solvent and its blended mixtures with a primary amine, secondary amine, and cyclical diamine were evaluated for the acid gas removal (AGR) process.

Although CA is one of the most effective methods for capturing CO₂, many challenges have been faced in modeling it accurately [18]. Equilibrium and non-equilibrium stage models are the two main approaches used to model CA processes. The traditional equilibrium approach is based on a well-recognized equilibrium stage model. In this method, vapor and liquid are assumed to enter a stage in a column, exchange matter and energy, and then leave in equilibrium with each other. It is assumed that equilibrium exists between the vapor and liquid at different stages [19]. However, in the rate-based (RB) model, mechanical, chemical, and thermodynamic equilibria are assumed to exist only at the fluid interface [20]. Accordingly, in addition to the equations related to equilibrium modeling, the mass and heat transfer rate equations are solved. Furthermore, the rigorous RB model considers reaction kinetics, film discretization with several segments, and electrolyte thermodynamics [21]. This allows the RB method to avoid efficiency approximation, as in the equilibrium method [22]. In addition to the mass and heat transfer rates, transfer coefficients, hydrodynamic equations, phase equilibria, and physical property models must be used in the RB model. Consequently, the RB model can provide more reliable results than the equilibrium stage model in column design [23,24]. In recent years, the non-equilibrium RB approach has taken over the standard equilibrium approach in gas absorber design for the CC process [25].

In this study, an industrial AGR process using amine-based solvents was simulated and designed using a systematic procedure for solvent selection. The AGR process was implemented based on post-combustion CC technology. First, various solvents were screened based on a literature review and preliminary simulations. Next, the absorption efficiency of each solvent was compared by modeling the absorber using the RB model. The electrolyte non-random two-liquid (E-NRTL) thermodynamic model was used to calculate the activity coefficient in the liquid phase, whereas the Redlich–Kwong (RK) equation of state was used for the gas phase. Potential candidates were then selected for the detailed simulation and design step. All processes were designed on an industrial scale and simulated using the commercial simulator Aspen Plus version 12.1 (© Aspen Technology Inc., Bedford, MA, USA). Then, the energy requirement and economic and environmental impacts of all processes were assessed and compared. A sensitivity analysis was also performed. Accordingly, the most promising solvents and a detailed design of the AGR process on a large scale could be investigated through a systematic procedure.

2. Methods

2.1. Systematic Procedure for Absorbent Selection

Selecting an effective absorbent is critical in the design of the AGR process. The absorbent should not only have a high absorption efficiency and low toxicity but should also provide energy-effective absorbent regeneration. Figure 2 shows the proposed schematic flowsheet of the absorbent selection for the absorber-regeneration configuration. First, a list of potential absorbents was identified by conducting a literature review. Next, the absorber column was modeled using the RB method in Aspen Plus. All solvents were tested and compared in terms of their absorption efficiency. A shortened list of absorbents was selected for the detailed design step. Herein, the entire absorber–regenerator configuration was simulated, designed, and optimized. The total energy requirement, total annual cost (TAC), and total CO₂ emissions (TEC) of all process alternatives were calculated and compared. Accordingly, the most promising absorbent and its optimal design was explored using this comprehensive solvent selection procedure.

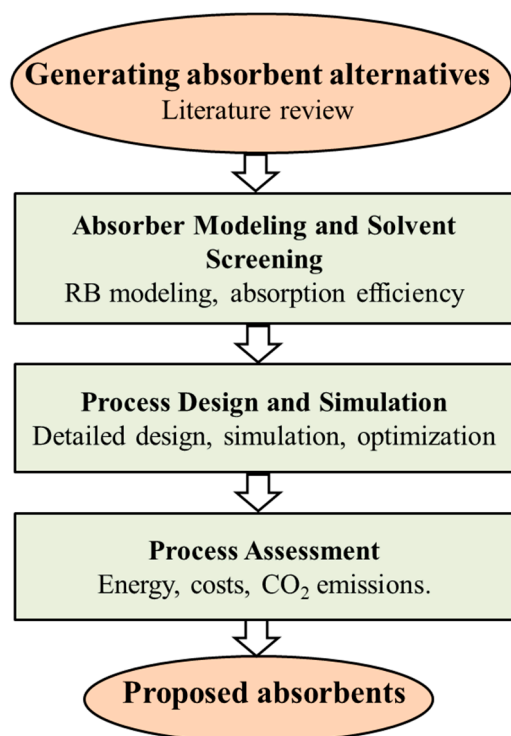


Figure 2. Systematic procedure of absorbent selection for AGR process.

2.2. Design and Simulation

The process simulation was conducted using the RadFrac model in Aspen Plus software. The important features of Aspen Plus are the availability of a large number of models for vapor–liquid equilibrium and calculation tools for achieving the convergence of the process flowsheet. For modeling the absorption column, RadFrac supports two approaches: equilibrium-based and rate-based; this study used the rate-based approach. This approach incorporates the two-film theory, which describes detailed mass transfer calculations. In the two-film theory, equilibrium is estimated at the interphase, and the mass transfer resistance between both phases is considered to calculate the overall resistance.

Thermodynamic modeling of the process plays a vital role in modeling and simulation studies. In this study, the E-NRTL thermodynamic model was used to calculate the activity coefficient in the liquid phase, whereas the RK equation of state was used for the gas phase. The E-NRTL model was applied for calculation as it is the most adaptable and appropriate electrolyte property method [24].

A mixed-flow model was used for rate-based modeling. In this model, the outlet conditions are similar to the bulk properties while leaving the stage. The details of this model are shown in Figure 3 [26]. A packed column typically provides a larger surface for absorption than a tray column. Therefore, Koch Flexipac corrugated sheet structured packing was used in the packed-bed absorption column, each a height of 12 m. The optimum value of column diameter was calculated according to the rate-based method for 85% of flooding and was taken as 6.6 and 6.2 m for A2 and A3 cases, respectively.

$x_{i,j}$			$x_{i,j}$
T_j^L	$x^{L,j}$	$y^{L,j}$	T_j^V
P_j	T_j	T_j	P_j
L_j			V_j
Bulk	Liquid	Vapor	Bulk
liquid	film	film	vapor

Figure 3. Rate-based mixed flow model.

The Scheffe-87 correlation was used to calculate the mass transfer coefficient and the interfacial area. For film discretization, the film reaction mode was specified so that reaction calculations could be performed.

2.3. Reactions and Kinetics

The equilibrium and kinetic reactions considered are as follows [27]:

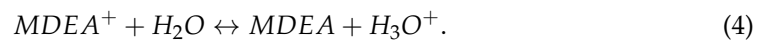
Dissociation of water:



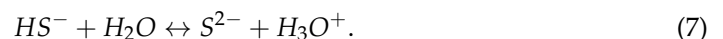
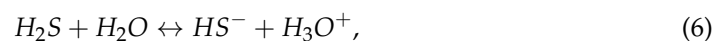
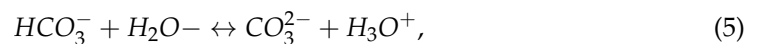
Dissolution of CO₂:



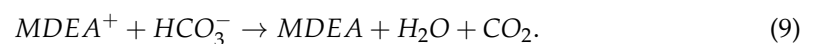
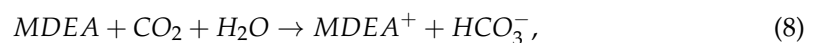
Dissociation of protonated amine:



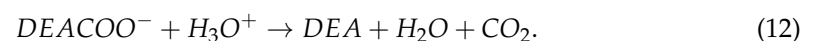
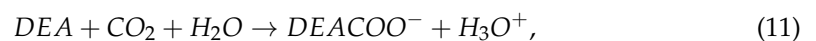
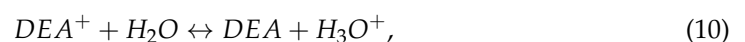
Dissociation of carbonate ion:



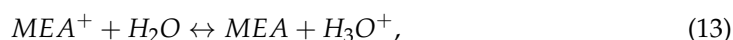
The mechanisms of the kinetic reactions, including CO₂ and MDEA, are presented in Equations (8) and (9).



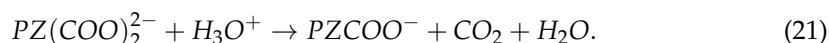
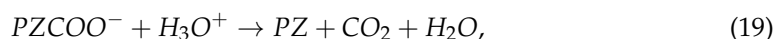
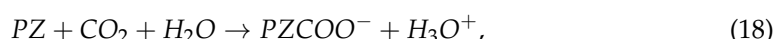
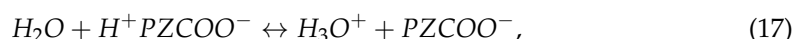
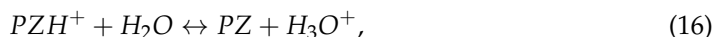
The following equilibrium and kinetic reactions occur when using a mixture of MDEA and DEA, in addition to previous reactions. The dissociation mechanism of protonated DEA occurs according to Equation (10). When DEA reacts with CO₂, carbamate is formed, and its mechanism is shown in Equations (11) and (12).



The mechanism for the dissociation of the protonated MEA occurs according to Equation (13). When MEA reacts with CO₂, carbamate is formed; this mechanism is shown in Equations (14) and (15).



PZ forms carbamate ions, zwitterions, and protonated carbamates in reaction with CO₂ [28,29].



Chemical absorption of CO₂ in primary and secondary amines occurs according to the zwitterion mechanism. This mechanism involves the generation of zwitterions, which then transform into carbamate ions through deprotonation. The time-resolved absorption spectroscopy is a reliable analysis method to investigate the depth of the reaction rate and absorption process [30,31]. The kinetic parameters of CO₂ absorption by all amines in this study were taken from the literature and are presented in Table 1 [15,24].

Table 1. Kinetic parameters of CO₂ absorption by different absorbents.

No.	Reactions	Reaction Rate	Activation Energy J/kmol
1	$\text{CO}_2 + \text{OH}^- \rightarrow \text{HCO}_3^-$	4.32×10^{13}	5.55×10^7
2	$\text{HCO}_3^- \rightarrow \text{CO}_2 + \text{OH}^-$	2.38×10^{17}	1.23×10^8
3	$\text{MDEA} + \text{CO}_2 + \text{H}_2\text{O} \rightarrow \text{MDEA}^+ + \text{HCO}_3^-$	2.22×10^7	3.78×10^7
4	$\text{MDEA}^+ + \text{HCO}_3^- \rightarrow \text{MDEA} + \text{H}_2\text{O} + \text{CO}_2$	1.06×10^{16}	1.06×10^8
5	$\text{DEA} + \text{CO}_2 + \text{H}_2\text{O} \rightarrow \text{DEACOO}^- + \text{H}_3\text{O}^+$	6.48×10^{16}	2.12×10^7
6	$\text{DEACOO}^- + \text{H}_3\text{O}^+ \rightarrow \text{DEA} + \text{H}_2\text{O} + \text{CO}_2$	1.43×10^{17}	4.81×10^7
7	$\text{MEA} + \text{CO}_2 + \text{H}_2\text{O} \rightarrow \text{MEACOO}^- + \text{H}_3\text{O}^+$	9.77×10^{10}	4.13×10^7
8	$\text{MEACOO}^- + \text{H}_3\text{O}^+ \rightarrow \text{MEA} + \text{H}_2\text{O} + \text{CO}_2$	2.08×10^{18}	5.92×10^7
9	$\text{PZ} + \text{CO}_2 + \text{H}_2\text{O} \rightarrow \text{PZCOO}^- + \text{H}_3\text{O}^+$	4.14×10^{10}	3.36×10^7
10	$\text{PZCOO}^- + \text{H}_3\text{O}^+ \rightarrow \text{PZ} + \text{CO}_2 + \text{H}_2\text{O}$	7.94×10^{21}	6.59×10^7
11	$\text{PZCOO}^- + \text{CO}_2 + \text{H}_2\text{O} \rightarrow \text{PZ}(\text{COO})_2^{2-} + \text{H}_3\text{O}^+$	3.62×10^{10}	3.36×10^7
12	$\text{PZ}(\text{COO})_2^{2-} + \text{H}_3\text{O}^+ \rightarrow \text{PZCOO}^- + \text{CO}_2 + \text{H}_2\text{O}$	5.56×10^{25}	7.68×10^7

2.4. Techno-Economic and Environmental Assessment

For a fair comparison of the economic impact, the total investment cost (TIC), total operating cost (TOC), and TAC of all process alternatives were estimated as described in previous studies [32]. Equipment costs were estimated using correlations from Turton et al. and Biegler et al. [33,34]. The TIC calculation was updated using the 2020 Chemical Engineering Index of 596.2. Heat exchangers, condensers, reboilers, tray stacks, and column vessels were considered in the TIC. A cooling water price of USD 0.35/GJ and a low-pressure steam price of USD 13.28/GJ were used for the TOC calculations [34]. A plant lifetime of 10 years was assumed, and a fixed interest rate of 8% was used for the TAC estimates.

The total annual CO₂ emissions (TCE) of all processes were calculated for the environmental assessment. Gadalla's method was used to calculate the CO₂ emissions from steam reboilers [35]:

$$[\text{CO}_2]_{emiss} = \left(\frac{Q_{fuel}}{NHV} \right) \left(\frac{C\%}{100} \right) \alpha, \quad (22)$$

where NHV is the net heating value of the fuel and $C\%$ is the carbon content. The molar mass ratio of CO₂ to C was $\alpha = 3.67$. Q_{fuel} , which denotes the amount of fuel used, is calculated as follows:

$$Q_{fuel} = \left(\frac{Q_{proc}}{\lambda_{proc}} \right) (h_{proc} - 419) \left(\frac{T_{FTB} - T_0}{T_{FTB} - T_{stack}} \right), \quad (23)$$

where Q_{proc} is the required heat duty of the system, λ_{proc} (kJ/kg) is the latent heat, and h_{proc} (kJ/kg) is the enthalpy of steam. The flame temperature (T_{FTB}) was 1800 °C, stack temperature (T_{stack}) was 160 °C, and ambient temperature (T_0) was 25 °C.

3. Results and Discussions

In this study, an industrial AGR process was designed based on the production rate of 900 kilotonnes of treated gas per year. A schematic diagram of the AGR, including the absorber and solvent regenerator, is shown in Figure 4. The feed mixture was a flue gas stream obtained from a post-combustion capture process. Table 2 lists the details of the feed conditions and the component compositions. Note that the H₂S concentration in the considered feed was higher than that in the typical flue gas. First, the flue gas feed and solvent were introduced into the absorber to generate a CO₂-rich solvent, H₂S at the bottom and a treated gas at the top. The rich solvent was then preheated by the lean recycling solvent and was delivered to the regenerator. Most of the CO₂ and H₂S were separated from the regenerator top stream, whereas the lean solvent was recycled to the absorber. The selection of an effective absorbent is critical in the design of the AGR process. In the following sections, various solvents are evaluated using the systematic procedure shown in Figure 2.

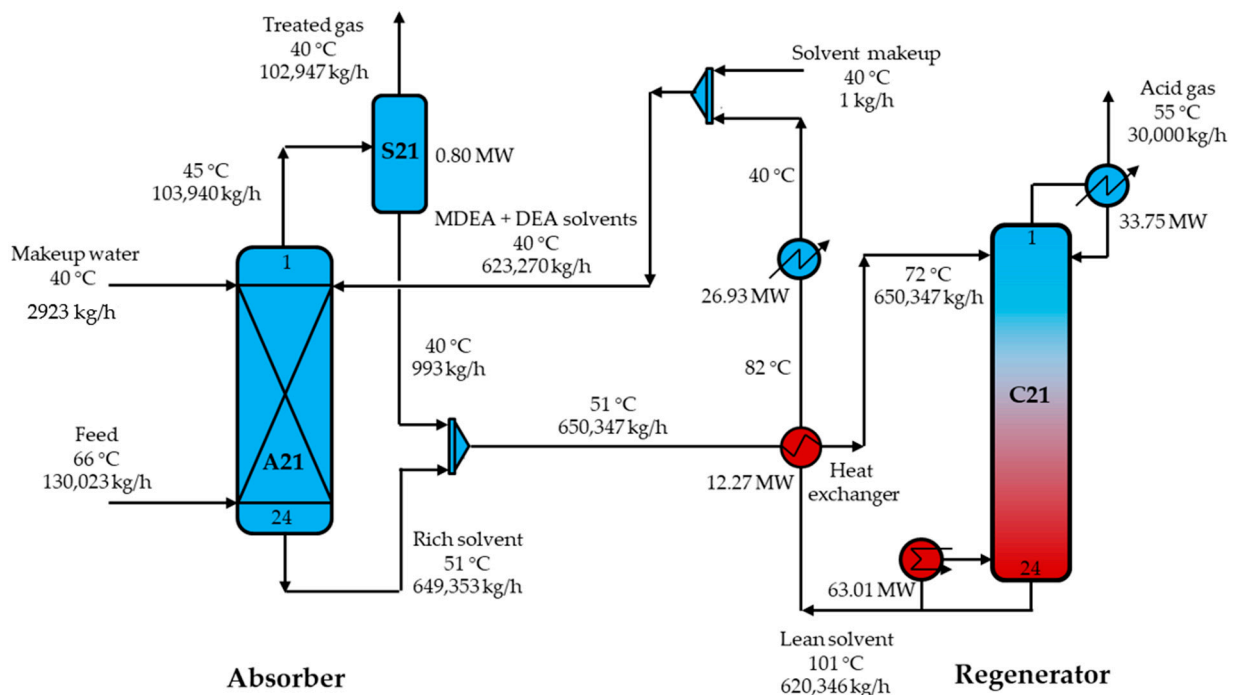


Figure 4. Schematic diagram of the AGR process using the blended solvent MDEA and DEA.

Table 2. Feed mixture conditions.

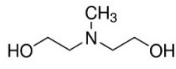
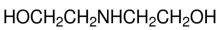
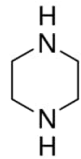
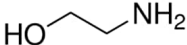
Component	Mass Fraction (wt%)
H ₂ O	2.40
CO ₂	19.35
H ₂ S	5.67
N ₂	72.58
Temperature (°C)	66
Pressure (bar)	1.2
Mass flowrate (kg/h)	130,023

3.1. Generating Absorbent Alternatives

In recent decades, aqueous solutions of alkanolamines have been widely used as absorbents in absorption processes to remove acidic gases from flue gas. MEA is the most commonly used chemical solvent to absorb CO₂ in the post-combustion CC process because of its fast reaction kinetics and high loading capacity at atmospheric pressure. In addition, MDEA is the only amine that is effective in absorbing H₂S and has a good equilibrium loading capacity and low heat of reaction with CO₂. Nonetheless, MDEA is a tertiary amine; it does not form carbamates with CO₂. Instead, mass transfer is influenced by the hydrolysis of CO₂ [12]. Recent studies have shown that a mixture of secondary and tertiary amines enhances the absorption efficiency of CO₂ [17]. MDEA and DEA have the highest CO₂ absorption fluxes compared to the MEA and PZ solutions studied in the literature. Recently, various studies have focused on CO₂ absorption in mixtures of MDEA and PZ [36,37]. PZ is commonly used as a promoter in amine mixtures [38]. The blended solution of MDEA and PZ provides resistance to thermal and oxidative degradation and reflects higher molecular interactions with CO₂ [29]. Blended solutions of MDEA and DEA had the highest CO₂ loading [15]. Many researchers use MEA as a benchmark. This study investigated amine-based absorbents that are commonly available, have widely available datasets, and whose properties are already incorporated in the Aspen Plus software. In particular, single amine solutions of tertiary amines (MDEA) and blended solutions of primary, secondary, and cyclical amines with tertiary amines were studied to investigate the effect of amine type.

A single-amine MDEA solution (A1) and different blended amine solutions (MDEA+DEA (A2), MDEA+PZ (A3), and MDEA+MEA (A4)) were used in this study. The details of the absorbents used in this study are listed in Table 3.

Table 3. Molecular formula and structures of absorbents used in this study.

Absorbents	Formula	Molecular Structures	Amine Type	CAS Number
N-Methyldiethanolamine (MDEA)	C ₅ H ₁₃ O ₂ N		Tertiary alkanolamine	105-59-9
Diethanolamine (DEA)	C ₄ H ₁₁ O ₂ N		Secondary alkanolamine	111-42-2
Piperazine (PZ)	C ₄ H ₁₀ N ₂		Cyclical diamine	110-85-0
Monoethanolamine (MEA)	C ₂ H ₇ ON		Primary alkanolamine	141-43-5

In this study, a tertiary amine solvent and its blended mixtures with a primary amine, a secondary amine, and a cyclical diamine were evaluated for the AGR process. In particular, four cases were evaluated.

- A1: Single-amine MDEA solution (30 wt% MDEA, 70 wt% H₂O);
- A2: Blends of MDEA and DEA solutions (15 wt% MDEA, 15 wt% DEA, and 70 wt% H₂O);
- A3: Blends of MDEA and PZ solutions (15 wt% MDEA, 15 wt% PZ, and 70 wt% H₂O);
- A4: Blends of MDEA and MEA solutions (15 wt% MDEA, 15 wt% MEA, and 70 wt% H₂O).

3.2. Absorber Modeling and Solvent Screening

In this step, the flue gas and the absorbent were input into the absorber, which was modeled by the RadFrac module in Aspen Plus. The E-NRTL thermodynamic model was used to calculate the activity coefficient in the liquid phase, whereas the RK equation of state was used for the gas phase. The absorber was modeled using a rate-based calculation method. A mixed flow model was selected, and film reactions were specified for both liquid and vapor phases. In the two-film theory, equilibrium is estimated at the interphase, and the mass transfer resistance between both phases is considered to calculate the overall resistance. The mass and heat transfer coefficients were predicted using the BRF-85 and Chilton–Colburn models, respectively. All reactions were input into the reaction set with the kinetic parameters listed in Table 1. To evaluate the absorption efficiency of the solvents, the feed flow rate of the flue gas was kept the same for all process alternatives, whereas the mass flow rate of the solvents was adjusted in each case. In particular, seven different feed-to-solvent mass ratios, 1:1, 1:1.5, 1:2, 1:2.5, 1:3, 1:3.5, and 1:4, were used to analyze the CO₂ and H₂S removal efficiencies in all cases.

Table 4 lists the results of CO₂ and H₂S removal efficiencies for all cases, i.e., A1, A2, A3, and A4. Note that in the A4 case, only four scenarios of feed-to-solvent ratios, i.e., 1:1, 1:1.5, 1:2, and 1:2.5, were examined as A4 can absorb mostly CO₂ (~100%) with the feed-to-solvent ratio of 1:2.5.

Table 4. CO₂ and H₂S removal efficiencies of different blended solvents.

Case	Feed/Solvent Ratio (Mass)	CO ₂ Removal Efficiency (wt%)	H ₂ S Removal Efficiency (wt%)
A1 (30 wt% MDEA)	1:1	15.0%	28.7%
	1:1.5	20.6%	43.0%
	1:2	24.6%	55.4%
	1:2.5	27.6%	65.8%
	1:3	30.2%	74.5%
	1:3.5	32.4%	81.9%
	1:4	34.5%	88.5%
A2 (15 wt% MDEA + 15 wt% DEA)	1:1	27.5%	15.4%
	1:1.5	40.3%	23.8%
	1:2	51.1%	32.9%
	1:2.5	60.1%	42.1%
	1:3	68.0%	50.8%
	1:3.5	75.0%	58.7%
	1:4	81.3%	65.8%
A3 (15 wt% MDEA + 15 wt% PZ)	1:1	39.4%	18.0%
	1:1.5	54.8%	30.0%
	1:2	67.0%	44.1%
	1:2.5	77.0%	60.4%
	1:3	86.0%	78.6%
	1:3.5	95.7%	95.5%
A4 (15 wt% MDEA + 15 wt% MEA)	1:1	43.0%	10.1%
	1:1.5	63.4%	15.0%
	1:2	82.4%	19.6%
	1:2.5	100.0%	23.4%

Figure 5 shows the effect of the solvent-to-feed ratio on the CO₂ absorption efficiency for the blended solvents considered. The simulation experiments showed that the CO₂ removal efficiency was ranked in the following order: A4 > A3 > A2 > A1. Among the four absorbents, case A1 produced unfavorable results as it could remove only 34.5 wt% of CO₂ from the gas feed with a solvent-to-feed ratio of 4. As a tertiary amine, MDEA does not have a hydrogen atom attached to nitrogen. Thus, it does not form carbamates with CO₂, resulting in low reactivity with CO₂ compared to other amines. However, when adding DEA, a secondary amine, to the MDEA mixture, the absorption efficiency was increased significantly, as in the case of A2. The MDEA + DEA solution can remove 81.3 wt% CO₂ from the flue gas with a solvent-to-feed ratio of 4. The higher reaction rate of DEA makes the MDEA + DEA solution much more favorable for absorbing CO₂. Remarkably, A4, which is a mixture of MDEA and MEA (a primary amine), showed the best performance, achieving a CO₂ absorption efficiency of nearly 100 wt% with a mass solvent-to-feed ratio of 2.5. Obviously, blends of tertiary amine (MDEA) and primary/secondary amines (MEA/DEA), which combine the higher reaction rate of MEA or DEA and the higher equilibrium capacity of MDEA, result in not only a considerable increase in CO₂ absorption efficiency but also a significant saving in energy requirements in the solvent regeneration stage. Note that because all blended solutions contain MDEA, the MDEA concentration of 15 wt% was fixed to make a fair comparison. In the case of blends of different solvents, we could vary the concentration of two amines in each mixture to achieve more detailed results.

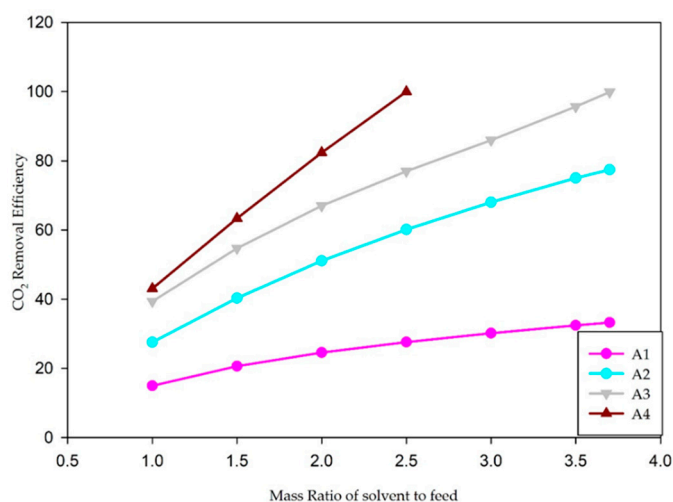


Figure 5. CO₂ removal efficiency vs. mass solvent-to-feed ratio for different solvents.

Figure 6 shows the effect of the solvent-to-feed ratio on H₂S removal efficiency for different cases. As the solvent-to-feed ratio was lower than 2.5, A1 showed the most favorable results for removing H₂S. As a tertiary amine, the main advantage of MDEA over other amines is its ability to selectively remove H₂S in the presence of CO₂. Therefore, MDEA has been widely utilized as a desulfurization solvent in the industry in recent years [36]. On the other hand, A4 presented unfavorable results for capturing H₂S, as less than 20 wt% H₂S was captured in the rich solvent stream. Adding MEA, a primary amine, to the MDEA solution reduced the H₂S absorption efficiency considerably compared to the single MDEA solution. Interestingly, A3 showed better performance in absorbing sulfur components than A1 when the solvent-to-feed ratio was greater than 3. Blends of MDEA and PZ can not only maintain the CO₂ absorption efficiency but also increase the H₂S absorption efficiency compared to every single solution.

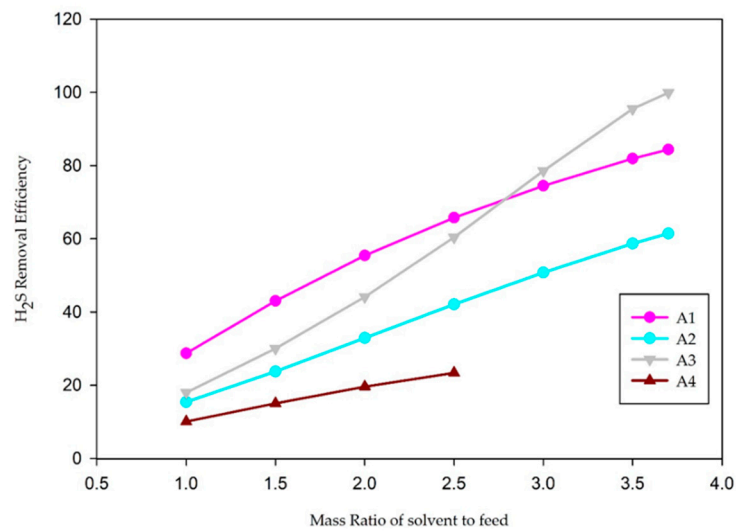


Figure 6. H₂S removal efficiency vs. mass solvent-to-feed ratio for different solvents.

Overall, MDEA has a high H₂S removal efficiency, but a very low CO₂ removal efficiency compared to its blends with other amines. On the contrary, blends of MDEA + MEA solutions have a high CO₂ absorption rate, but it was not favorable to remove H₂S. Therefore, A1 and A4 were not selected for the process design step. A2 (MDEA + DEA) and A3 (MDEA + PZ) not only provided favorable results for removing H₂S but also increased the CO₂ absorption efficiency significantly compared to the single MDEA solvent. Consequently, these two cases, A2 and A3, were selected to process design steps for detailed economic and environmental assessments.

The variation in the temperature profile along the absorber with the application of different types of amines as absorbents is shown in Figure 7.

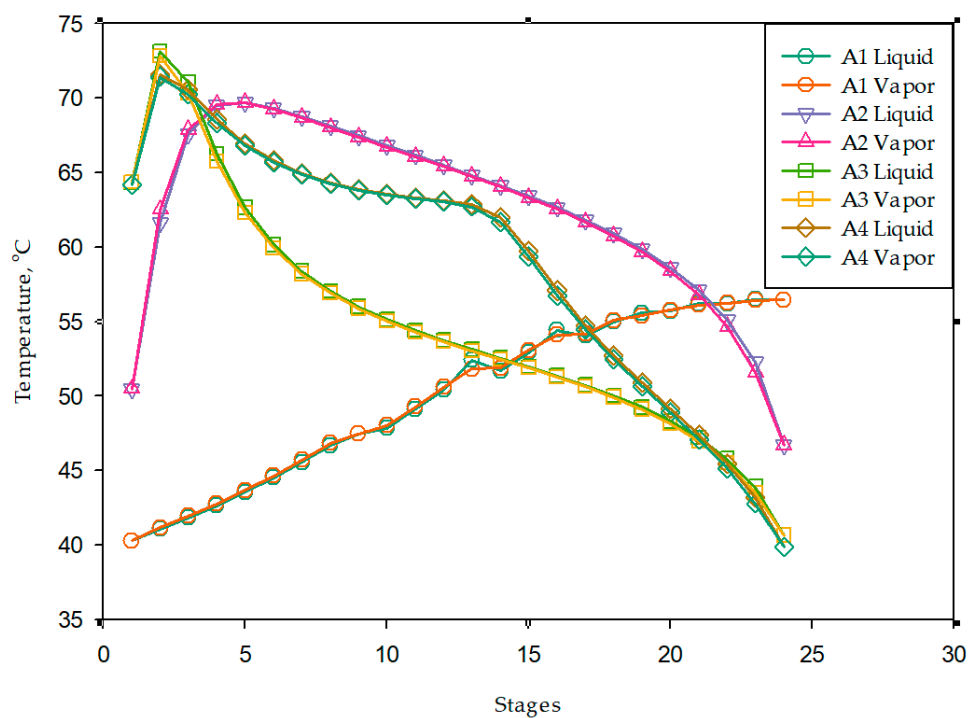


Figure 7. Variation in absorber temperature profile with the application of different types of amines as absorbents.

The interfacial temperature profile was equivalent to the liquid temperature profile in all cases, with temperature variation being directly related to the vapor heat transfer coefficients. It was found that there was a large difference in the absorption temperatures between the single and blended amine solutions. In the case of A2, the absorption temperature was the highest compared to the other cases, and it dropped at both edges; A3 exhibited the lowest absorption temperature. A temperature bulge was observed near the top of the column in all three blended amine solutions. Generally, the temperature profile of the absorption column reflects the reactions occurring at different stages. The composition of CO₂ in the absorbent is related to the reaction rate and equilibrium capacity of the CO₂ in the solvent [15].

The variations in the molar composition profile along the absorption column of the vapor stream of CO₂ with different absorbents are shown in Figure 8. The molar concentration of CO₂ in the vapor stream decreased as the fluid flowed towards the top of the column and came into contact with the absorbent. In particular, A1 showed the lowest CO₂ absorption efficiency as the CO₂ concentration in vapor phase remained at a high level from stage 25 to stage 11. This is because MDEA is a tertiary amine, which does not form carbamates with CO₂. In cases of A2 and A3, the CO₂ vapor fractions decreased gradually along the absorber. Interestingly, the CO₂ vapor concentration in A4 reduced dramatically at the middle of the absorber, and it only reached the required target in stage 12. In fact, the MDEA + MEA solution achieved a CO₂ absorption efficiency of nearly 100 wt% with a mass solvent-to-feed ratio of 2.5.

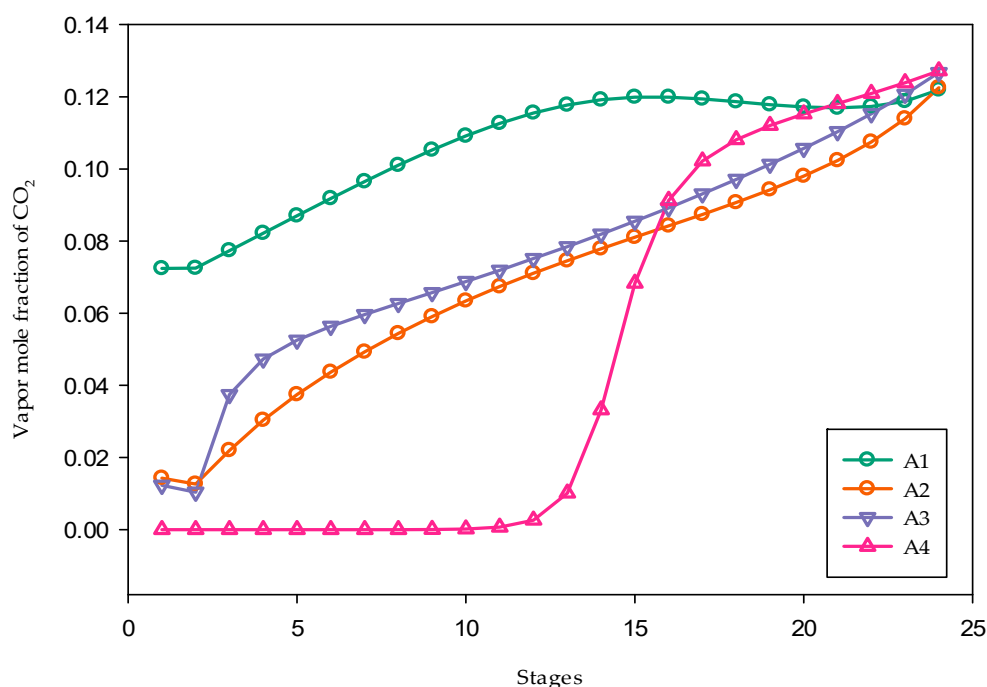


Figure 8. Variation in molar composition profile of CO₂ in vapor stream with the application of different types of amines as absorbents.

3.3. Process Design

In the following sections, the processes of two promising absorbents, i.e., A2 (solution of MDEA + DEA) and A3 (solution of MDEA + PZ), were designed, optimized, and evaluated in detail. The absorbent and flue gas feed were counter-currently introduced into the absorber to produce a solvent-rich stream containing most of the acid gases at the bottom and a treated gas stream at the top. CO₂ and H₂S were solubilized and absorbed in solvent solutions through chemical reactions, as mentioned in Section 2.3. To make a fair comparison, the solvent-to-feed mass ratio in each process was specified to remove more than 90 wt% CO₂ from the flue gas. The rich solvent stream was then input into the

stripper to regenerate the lean solvent. In all cases, the regenerator column was designed to achieve a CO₂ recovery of at least 99.7 wt%. All distillation columns were optimized to minimize TAC by varying the total number of stages and feed locations while maintaining the product purities and recoveries. The optimization procedure was described in detail in prior research [39].

3.3.1. MDEA-DEA Absorbent Process

Figure 4 depicts the key design parameters and stream information of the optimized AGR process using a blended solution of MDEA and DEA. The feed and the MDEA + DEA solution were introduced counter-currently into the absorber from the bottom and top, respectively. In the absorber, acid gases such as CO₂ and H₂S were solubilized and absorbed by the solvent. The treated gas from the A21 top was sent to the knockout drum to isolate water before leaving the process. A solvent-to-feed mass ratio of 4.8 was specified to achieve a CO₂ removal efficiency of 90 wt%. The solvent-rich stream from the A21 bottom was then preheated by the lean solvent to 72 °C before being input into a distillation column (C21), called a solvent regenerator, to separate the acid gases at the top and the lean solvent at the bottom. Herein, 99.7 wt% of CO₂ in the rich solvent stream was delivered as the C21 overhead, while the lean solvent was sent to the bottom. To improve the process heat recovery, the lean solvent was exchanged and heated with the regenerator feed before being cooled to 40 °C and was introduced back to the absorber. A make-up solvent of 1 kg/h and water of 2923 kg/h were added to account for small losses of solvent and water, respectively, in the process. The simulation results showed that energies of 63.01 and 33.75 MW were required in the C21 reboiler and condenser, respectively. Note that the low-pressure steam (5 bar, 160 °C) was used for the C21 reboiler.

3.3.2. MDEA-PZ Absorbent Process

Figure 9 shows the key design parameters and stream information of the optimized AGR process using a blended solution of MDEA and PZ. First, the flue gas feed was input into the absorber (A31) bottom, whereas the blend solution of MDEA + PZ was introduced to the A31 top to carry out chemical absorption. Next, the acid gases were solubilized into the solvent solution by reactions (2), (3), (6), and (7), while MDEA and PZ reacted with CO₂ through reactions (8), (9), and (16–21) mentioned in Section 2.3. PZ formed carbamate ions, zwitterions, and protonated carbamates upon reaction with CO₂. To achieve a CO₂ removal efficiency of 90 wt%, the mass ratio solvent-to-feed of 3.2 was specified. At the A31 top, the treated gas was introduced into the knockout drum to separate water before leaving the AGR process. Meanwhile, at the A31 bottom, the solvent-rich stream was then heated from the recycled lean solvent stream to 64 °C before being sent to a stripper (C31). C31 was designed to isolate more than 99.7 wt% of CO₂ in the rich solvent stream to the C21 overhead. The C31 bottom stream released heat to the C31 feed to reduce heat loss before being cooled to 40 °C to recycle back to the absorber. Make-up water of 2657 kg/h was added to account for a small loss of water during the process. The simulation results showed that the energy requirements for the C31 reboiler and condenser were 43.89 and 25.65 MW, respectively. It is noteworthy that because MDEA + PZ has a better performance for CO₂ absorption, the required solvent flow rate of MDEA + PZ was 32.9% less than the required MDEA + DEA flow rate. Accordingly, the MDEA + PZ solvent process can save up to 30.3% of the energy required in the reboiler compared to the MDEA + DEA solvent process.

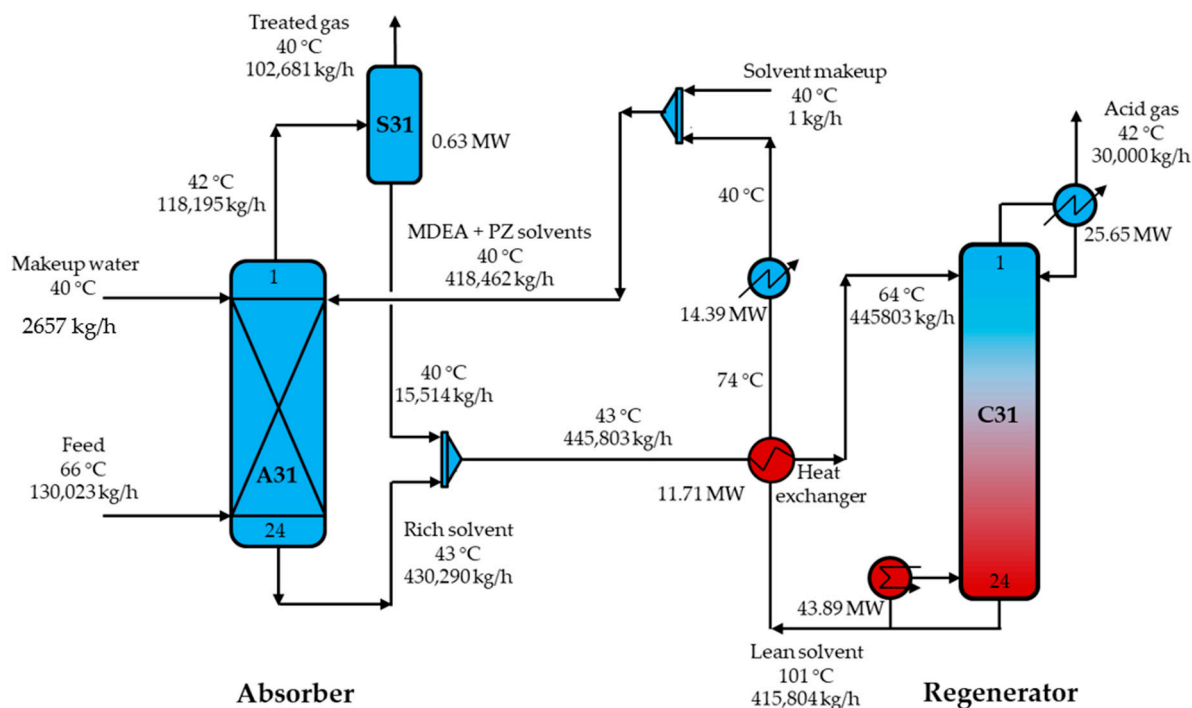


Figure 9. Schematic diagram of the AGR process using the blended solvent MDEA and PZ.

Table 5 lists the key results for all process alternatives, including energy requirements, TIC, TOC, TAC, and carbon emissions. Remarkably, the MDEA + PZ solvent process showed the most promising results in reducing the TIC and TOC up to 10.1% and 30.4%, respectively, compared to the MDEA + DEA solvent process. Consequently, the MDEA + PZ process can save up to 29.1% of TAC compared to the MDEA + DEA process. As energy consumption is closely linked to carbon emissions, the MDEA + PZ process was much more environmentally friendly, reducing 30.3% of the carbon footprint relative to the MDEA + DEA process.

Table 5. Comparison of AGR processes using different absorbents.

Structural Alternative	A2 (MDEA + DEA)	A3 (MDEA + PZ)
Reboiler duties (MW)	63.01	43.89
Reboiler duty savings		30.3%
Condenser duties (MW)	68.68	40.69
Condenser duty savings		40.8%
TIC (US k\$)	12,451	11,194
TIC savings		10.1%
TOC (US k\$/year)	26,009	18,093
TOC savings		30.4%
TAC (US k\$/year)	27,865	19,761
TAC savings		29.1%
TCE (ton/year)	128,528	89,527
TCE reduction		30.3%

The results showed that the blend of MDEA and PZ solution was the most promising absorbent for capturing CO₂ and H₂S from flue gas. The proposed process design and operating conditions can be recommended for both retrofitting and grassroots projects. In particular, retrofitting can be easily accomplished with a short modification time owing to the standard design of the chemical absorption process.

Figure 10 compares the removal efficiency of CO₂ in all considered solvents in this study to that reported in recent literature [24,40–43]. As a single tertiary amine, MDEA

solvent attained the lowest CO₂ absorption efficiency of 34.5%. However, the blended solutions of MDEA + DEA showed better performance with 90.0% and 65.8% of CO₂ and H₂S absorption efficiencies, respectively. Remarkably, the MDEA + PZ solution could absorb up to 99.99% of CO₂ and 99.99% of H₂S in the flue gas as the mass solvent-to-feed ratio is greater than 4. This can be attributed to the formation of carbamate and the high heat of the reaction.

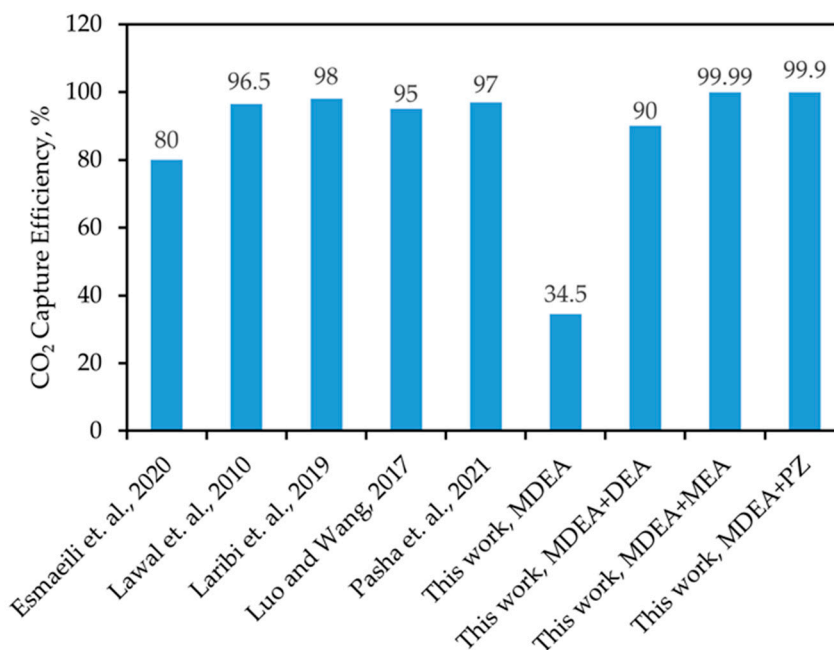


Figure 10. Comparison of CO₂ capture efficiency with literature [24,40–43].

4. Conclusions

In this study, rigorous simulation and design of an industrial acid gas removal (AGR) process using amine-based solvents was successfully developed. The most promising absorbent was explored through a systematic procedure for solvent selection, including both solvent screening and process design steps. To the best of our knowledge, this is the first study demonstrating the selection of blended amine solutions for the AGR process, which carried out two steps: solvent screening using rate-based modeling and detailed process design on an industrial scale.

Various amine-based solvents were screened for their CO₂ and H₂S absorption efficiencies. Two promising blend solutions, MDEA + DEA and MDEA + PZ, were selected for the process-design step. All simulations were performed using the Aspen Plus software. The E-NRTL thermodynamic model was used to calculate the activity coefficient in the liquid phase, whereas the RK equation of state was used for the gas phase. The absorption column was reliably modeled using a non-equilibrium rate-based method. For a holistic comparison, the techno-economic and environmental impacts of all processes were assessed. The blend of MDEA + PZ was found to be the most suitable absorbent for the studied AGR process because the process could save up to 10.1% of TIC and 29.1% of TAC compared to the MDEA + DEA solvent process. Furthermore, 30.3% of carbon emissions could be reduced using MDEA + PZ solution relative to the process using MDEA + DEA solutions. The proposed AGR process is especially promising for retrofitting projects with a short implementation time.

Author Contributions: N.A. and L.C.N. contributed equally to this work by designing the study, performing process simulations, and writing the article. M.L. conceived of the core research concepts and advised academically. All authors have read and agreed to the published version of the manuscript.

Funding: This work was supported by the 2022 Yeungnam University Research Grant and the Priority Research Centers Program through the National Research Foundation (NRF) of Korea, funded by the Ministry of Education (2014R1A6A1031189).

Data Availability Statement: Not applicable.

Conflicts of Interest: The authors declare no conflict of interest.

References

1. Masson-Delmotte, V.; Zhai, P.; Chen, Y.; Goldfarb, L.; Gomis, M.I.; Matthews, J.B.R.; Berger, S.; Huang, M.; Yelekçi, O.; Yu, R.; et al. *Climate Change 2021: The Physical Science Basis Contribution of Working Group I to the Sixth Assessment Report of the Intergovernmental Panel on Climate Change*; IPCC: Geneva, Switzerland, 2021; ISBN 9789291691586.
2. Carbon Dioxide. Available online: <https://climate.nasa.gov/vital-signs/carbon-dioxide/> (accessed on 18 April 2022).
3. Carbon Capture. Available online: <https://www.c2es.org/content/carbon-capture/> (accessed on 28 May 2022).
4. Ishaq, H.; Ali, U.; Sher, F.; Anus, M.; Imran, M. Process analysis of improved process modifications for ammonia-based post-combustion CO₂ capture. *J. Environ. Chem. Eng.* **2021**, *9*, 104928. [CrossRef]
5. Ma'mun, S.; Svendsen, H.F.; Bendiyasa, I.M. Amine-based carbon dioxide absorption: Evaluation of kinetic and mass transfer parameters. *J. Mech. Eng. Sci.* **2018**, *12*, 4088–4097. [CrossRef]
6. Peng, Y.; Zhao, B.; Li, L. Advance in Post-Combustion CO₂ Capture with Alkaline Solution: A Brief Review. *Energy Procedia* **2012**, *14*, 1515–1522. [CrossRef]
7. Borhani, T.N.G.; Akbari, V.; Afkhamipour, M.; Hamid, M.K.A.; Manan, Z.A. Comparison of equilibrium and non-equilibrium models of a tray column for post-combustion CO₂ capture using DEA-promoted potassium carbonate solution. *Chem. Eng. Sci.* **2015**, *122*, 291–298. [CrossRef]
8. Hospital-Benito, D.; Lemus, J.; Moya, C.; Santiago, R.; Ferro, V.R.; Palomar, J. Techno-economic feasibility of ionic liquids-based CO₂ chemical capture processes. *Chem. Eng. J.* **2021**, *407*, 127196. [CrossRef]
9. Fu, K.; Liu, C.; Wang, L.; Huang, X.; Fu, D. Performance and mechanism of CO₂ absorption in 2-ethylhexan-1-amine + glyme non-aqueous solutions. *Energy* **2021**, *220*, 119735. [CrossRef]
10. Jung, W.; Lee, J. Thermodynamic and kinetic modeling of a novel polyamine-based solvent for energy-efficient CO₂ capture with energy analysis. *Energy* **2022**, *239*, 122347. [CrossRef]
11. Jung, W.; Kim, E.; Lee, J.; Lee, K.S. Design of a water wash column in the CO₂ capture process using a polyamine-based water-lean solvent. *J. Nat. Gas Sci. Eng.* **2021**, *95*, 104204. [CrossRef]
12. Moioli, S.; Pellegrini, L.A.; Picutti, B.; Vergani, P. Improved rate-based modeling of H₂S and CO₂ removal by methyldiethanolamine scrubbing. *Ind. Eng. Chem. Res.* **2013**, *52*, 2056–2065. [CrossRef]
13. Sheng, M.; Xie, C.; Zeng, X.; Sun, B.; Zhang, L.; Chu, G.; Luo, Y.; Chen, J.F.; Zou, H. Intensification of CO₂ capture using aqueous diethylenetriamine (DETA) solution from simulated flue gas in a rotating packed bed. *Fuel* **2018**, *234*, 1518–1527. [CrossRef]
14. El Hadri, N.; Quang, D.V.; Goetheer, E.L.V.; Abu Zahra, M.R.M. Aqueous amine solution characterization for post-combustion CO₂ capture process. *Appl. Energy* **2017**, *185*, 1433–1449. [CrossRef]
15. Esmaeili, A.; Liu, Z.; Xiang, Y.; Yun, J.; Shao, L. Simulation and validation of carbon dioxide removal from the ethane stream in the south pars phase 19 gas plant by different amine solutions using rate-based model. *J. Nat. Gas Sci. Eng.* **2021**, *93*, 104030. [CrossRef]
16. Kalatjari, H.R.; Haghtalab, A.; Nasr, M.R.J.; Heydarinasab, A. Experimental, simulation and thermodynamic modeling of an acid gas removal pilot plant for CO₂ capturing by mono-ethanol amine solution. *J. Nat. Gas Sci. Eng.* **2019**, *72*, 103001. [CrossRef]
17. Rivera-Tinoco, R.; Bouallou, C. Comparison of absorption rates and absorption capacity of ammonia solvents with MEA and MDEA aqueous blends for CO₂ capture. *J. Clean. Prod.* **2010**, *18*, 875–880. [CrossRef]
18. Fang, M.; Zhu, D. Chemical Absorption. In *Handbook of Climate Change Mitigation and Adaptation*; Springer: New York, NY, USA, 2015; pp. 1–109.
19. Seader, J.D.; Henley, E.J.; Roper, D.K. *Separations Process Principles. Chemical and Biochemical Operations*, 3rd ed.; John Wiley & Son, Inc.: New York, NY, USA, 2011; ISBN 9780470481837.
20. Ross Taylor, R.K. *Multicomponent Mass Transfer*; Wiley: New York, NY, USA, 1993; ISBN 978-0-471-57417-0.
21. Kenig, E.Y.; Schneider, R.; Górak, A. Reactive absorption: Optimal process design via optimal modelling. *Chem. Eng. Sci.* **2001**, *56*, 343–350. [CrossRef]
22. Krishnamurthy, R.; Taylor, R. Absorber simulation and design using a nonequilibrium stage model. *Can. J. Chem. Eng.* **1986**, *64*, 96–105. [CrossRef]
23. Zhang, Y.; Chen, C.C. Modeling CO₂ absorption and desorption by aqueous monoethanolamine solution with Aspen rate-based model. *Energy Procedia* **2013**, *37*, 1584–1596. [CrossRef]
24. Esmaeili, A.; Liu, Z.; Xiang, Y.; Yun, J.; Shao, L. Modeling and validation of carbon dioxide absorption in aqueous solution of piperazine + methyldiethanolamine by PC-SAFT and e-NRTL models in a packed bed pilot plant: Study of kinetics and thermodynamics. *Process Saf. Environ. Prot.* **2020**, *141*, 95–109. [CrossRef]

25. Salvinder, K.M.S.; Zabiri, H.; Isa, F.; Taqvi, S.A.; Roslan, M.A.H.; Shariff, A.M. Dynamic modelling, simulation and basic control of CO₂ absorption based on high pressure pilot plant for natural gas treatment. *Int. J. Greenh. Gas Control* **2018**, *70*, 164–177. [[CrossRef](#)]
26. Zhang, Y.; Chen, H.; Chen, C.C.; Plaza, J.M.; Dugas, R.; Rochelle, G.T. Rate-based process modeling study of CO₂ Capture with aqueous monoethanolamine solution. *Ind. Eng. Chem. Res.* **2009**, *48*, 9233–9246. [[CrossRef](#)]
27. Zhang, Y.; Chen, C.C. Thermodynamic modeling for CO₂ absorption in aqueous MDEA solution with electrolyte NRTL model. *Ind. Eng. Chem. Res.* **2011**, *50*, 163–175. [[CrossRef](#)]
28. Zhao, B.; Liu, F.; Cui, Z.; Liu, C.; Yue, H.; Tang, S.; Liu, Y.; Lu, H.; Liang, B. Enhancing the energetic efficiency of MDEA/PZ-based CO₂ capture technology for a 650 MW power plant: Process improvement. *Appl. Energy* **2017**, *185*, 362–375. [[CrossRef](#)]
29. Sharif, M.; Zhang, T.; Wu, X.; Yu, Y.; Zhang, Z. Evaluation of CO₂ absorption performance by molecular dynamic simulation for mixed secondary and tertiary amines. *Int. J. Greenh. Gas Control* **2020**, *97*, 103059. [[CrossRef](#)]
30. Wang, C.; Liu, Y.; Guo, Y.; Ma, L.; Liu, Y.; Zhou, C.; Yu, X.; Zhao, G. Lead-free sodium bismuth halide Cs₂NaBiX₆ double perovskite nanocrystals with highly efficient photoluminescence. *Chem. Eng. J.* **2020**, *397*, 125367. [[CrossRef](#)]
31. Wang, C.; Ma, L.; Wang, S.; Zhao, G. Efficient Photoluminescence of Manganese-Doped Two-Dimensional Chiral Alloyed Perovskites. *J. Phys. Chem. Lett.* **2021**, *12*, 12129–12134. [[CrossRef](#)] [[PubMed](#)]
32. Nhien, L.C.; Long, N.V.D.; Kim, S.; Lee, M. Design and optimization of intensified biorefinery process for furfural production through a systematic procedure. *Biochem. Eng. J.* **2016**, *116*, 166–175. [[CrossRef](#)]
33. Biegler, L.T.; Grossmann, I.E.; Westerberg, A.W. *Systematic Methods of Chemical Process Design*; Prentice Hall Inc.: Hoboken, NJ, USA, 1997.
34. Turton, R.; Bailie, R.C.; Whiting, W.B.; Shaeiwitz, J.A.; Bhattacharyya, D. *Analysis, Synthesis, and Design of Chemical Processes*, 4th ed.; Prentice Hall: Hoboken, NJ, USA, 2016.
35. Gadalla, M.A.; Olujic, Z.; Jansens, P.J.; Jobson, M.; Smith, R. Reducing CO₂ emissions and energy consumption of heat-integrated distillation systems. *Environ. Sci. Technol.* **2005**, *39*, 6860–6870. [[CrossRef](#)] [[PubMed](#)]
36. Moioli, S.; Pellegrini, L.A. Modeling the methyldiethanolamine-piperazine scrubbing system for CO₂ removal: Thermodynamic analysis. *Front. Chem. Sci. Eng.* **2016**, *10*, 162–175. [[CrossRef](#)]
37. Abdul Manaf, N.; Cousins, A.; Feron, P.; Abbas, A. Dynamic modelling, identification and preliminary control analysis of an amine-based post-combustion CO₂ capture pilot plant. *J. Clean. Prod.* **2016**, *113*, 635–653. [[CrossRef](#)]
38. Prentza, L.; Koronaki, I.P.; Nitsas, M.T. Investigating the performance and thermodynamic efficiency of CO₂ reactive absorption—A solvent comparison study. *Therm. Sci. Eng. Prog.* **2018**, *7*, 33–44. [[CrossRef](#)]
39. Nhien, L.C.; Long, N.V.D.; Kim, S.; Lee, M. Design and Assessment of Hybrid Purification Processes through a Systematic Solvent Screening for the Production of Levulinic Acid from Lignocellulosic Biomass. *Ind. Eng. Chem. Res.* **2016**, *55*, 5180–5189. [[CrossRef](#)]
40. Lawal, A.; Wang, M.; Stephenson, P.; Koumpouras, G.; Yeung, H. Dynamic modelling and analysis of post-combustion CO₂ chemical absorption process for coal-fired power plants. *Fuel* **2010**, *89*, 2791–2801. [[CrossRef](#)]
41. Laribi, S.; Dubois, L.; De Weireld, G.; Thomas, D. Study of the post-combustion CO₂ capture process by absorption-regeneration using amine solvents applied to cement plant flue gases with high CO₂ contents. *Int. J. Greenh. Gas Control* **2019**, *90*, 102799. [[CrossRef](#)]
42. Luo, X.; Wang, M. Improving Prediction Accuracy of a Rate-Based Model of an MEA-Based Carbon Capture Process for Large-Scale Commercial Deployment. *Engineering* **2017**, *3*, 232–243. [[CrossRef](#)]
43. Pasha, M.; Li, G.; Shang, M.; Liu, S.; Su, Y. Mass transfer and kinetic characteristics for CO₂ absorption in microstructured reactors using an aqueous mixed amine. *Sep. Purif. Technol.* **2021**, *274*, 118987. [[CrossRef](#)]